



## Article

# The Effect of Shear Deformation on C-N Structure under Pressure up to 80 GPa

Valentin Churkin <sup>1,2</sup>, Boris Kulnitskiy <sup>1,2</sup>, Pavel Zinin <sup>3,\*</sup>, Vladimir Blank <sup>1,2,4</sup> and Mikhail Popov <sup>1,2,4,\*</sup>

<sup>1</sup> Technological Institute for Superhard and Novel Carbon Materials, Centralnaya Str. 7a, Troitsk, 142190 Moscow, Russia; churkin\_valentin@rambler.ru (V.C.); boris@tisnum.ru (B.K.); vblank@tisnum.ru (V.B.)

<sup>2</sup> Moscow Institute of Physics and Technology State University, Institutskiy per. 9, Dolgoprudny, 141700 Moscow, Russia

<sup>3</sup> Scientific and Technological Center of Unique Instrumentation, Russian Academy of Sciences, Butlerova str. 15, 117342 Moscow, Russia

<sup>4</sup> Research Centre, National University of Science and Technology MISiS, Leninskiy prospekt 4, 119049 Moscow, Russia

\* Correspondence: zosimpvz@mail.ru (P.Z.); mikhail.popov@tisnum.ru (M.P.)

**Abstract:** We study the effect of shear deformation on graphitic  $g\text{-C}_3\text{N}_4$  under pressures of up to 80 GPa at room temperature.  $g\text{-C}_3\text{N}_4$  samples are transformed from initial amorphous flakes into onion-like structures, in which the nitrogen content in the quenched samples decreases with increasing pressure (from 42% in the initial conditions to 1% at 80 GPa). The concentration of the  $sp^2$  bonds also decreases from 1 (the initial sample) to 0.62 with increasing pressure to 80 GPa. This transformation of the sample is due to the fact that in the pressure range of 55–115 GPa, the equilibrium phase is not a diamond, but instead, carbon onions cross-linked by  $sp^3$  bonds, which are denser than diamonds. The results of our study show that the presence of nitrogen in  $sp^3$ -bonded structures at pressures of higher than 55 GPa reduces the density and, accordingly, carbon structures without nitrogen become thermodynamically favorable.

**Keywords:**  $g\text{-C}_3\text{N}_4$ ; high pressure; phase diagram; onions



**Citation:** Churkin, V.; Kulnitskiy, B.; Zinin, P.; Blank, V.; Popov, M. The Effect of Shear Deformation on C-N Structure under Pressure up to 80 GPa. *Nanomaterials* **2021**, *11*, 828. <https://doi.org/10.3390/nano11040828>

Academic Editor:  
Diego Cazorla-Amorós

Received: 18 February 2021  
Accepted: 20 March 2021  
Published: 24 March 2021

**Publisher's Note:** MDPI stays neutral with regard to jurisdictional claims in published maps and institutional affiliations.



**Copyright:** © 2021 by the authors. Licensee MDPI, Basel, Switzerland. This article is an open access article distributed under the terms and conditions of the Creative Commons Attribution (CC BY) license (<https://creativecommons.org/licenses/by/4.0/>).

## 1. Introduction

According to recent experimental and computer modeling studies, fullerene-type onions cross-linked by  $sp^3$  bonds are the equilibrium phase of the carbon phase diagram at 55–115 GPa [1,2]. This discovery allows us to re-evaluate the phase diagram of C-N compounds from the perspective of obtaining new nanocluster-based materials. For many years, intense interest in the synthesis of new superhard materials has been generated by predictions on the unusual properties of saturated, i.e.,  $sp^3$ -hybridized, crystalline  $\text{C}_3\text{N}_4$ -phases [3]. Numerous attempts to obtain hypothetical phases have been undertaken since the Liu and Cohen publication. Despite many claims of making new  $\text{CN}_x$  films and  $\text{C}_3\text{N}_4$  crystallites, no convincing evidence has yet been obtained for the dense  $\text{C}_3\text{N}_4$  phases, other than graphite-like phases [4,5]. However, the synthesis of several new C-N-based phases [6–11], conducted recently, demonstrates how little is known about the behavior of C-N compounds under high pressure and indicates that the search for new high-pressure phases should be continued. Horvath-Bordon et al. [6] reported on high-pressure synthesis of a well-crystallized compound  $\text{C}_2\text{N}_2(\text{NH})$  with an N:C ratio of 3:2, in which all of the carbon atoms are tetrahedrally coordinated. The presence of structural hydrogen atoms was recognized (by nanoSIMS) and the composition of  $\text{C}_2\text{N}_2(\text{NH})$  was determined. The crystal structure of the new compound (defect-wurtzite  $d\text{wur-C}_2\text{N}_2(\text{NH})$ ) was determined by combining electron-diffraction results with primary principle theoretical studies. This finding was confirmed by Salamat et al. [12]. The crystal structure of carbon nitride under high pressure and temperature was investigated up to megabar pressures, using graphitic

$C_3N_4(g-C_3N_4)$  as a starting material. It transformed to an orthorhombic phase above 30 GPa and 1600 K, which has similar unit cell parameters to those of reported hydrogen-bearing carbon nitride phases, such as  $C_2N_2(NH)$  and  $C_2N_2(CH_2)$  [8]. These results suggest that in the studied wide pressure and temperature range, hydrogen-bearing carbon nitride favors an orthorhombic structure with a fundamental composition of  $C_2N_2X$ , where  $X = NH$  or  $CH_2$ . Another problem in achieving phase transition in a  $C_3N_4$  system relates to the fact that  $g-C_3N_4$  becomes transparent at high pressures [9,13] and, therefore, is difficult to heat by means of a laser to overcome the reaction activation barrier. For example, under hydrostatic conditions, graphite does not transform to diamond at pressures of less than 80 GPa [14], while activation of the phase transition by shear deformation leads to the direct transformation of graphite to diamond at pressures of 17–19 GPa at room temperature [1,2,15].

However, there is a way to overcome the reaction activation barrier by applying shear stress under high pressure [16,17]. In the present study, we investigate the effect of shear stress on the behavior of the C-N phase under high pressure, in the shear DAC (SDAC). Features of the activation of phase transitions in carbon nanocluster-based materials using SDAC were discussed in Reference [18].

## 2. Materials and Methods

Raman spectra were recorded with a Renishaw inVia Raman microscope (excitation wavelength 532 nm) (Renishaw plc, Spectroscopy Products Division, New Mills, Wotton-under-Edge, Gloucestershire GL12 8JR, United Kingdom). A high-resolution transmission electron microscopy (HRTEM) study was performed using a JEM 2010 TEM microscope (JEOL Ltd. 3-1-2 Musashino, Akishima, Tokyo 196-8558, Japan) with a GIF Quantum attachment for EELS. (DigitalMicrograph, Gatan's software, GATAN: 5794 W. Las Positas Blvd. Pleasanton, CA 94588, United States) for transmission electron microscopy (TEM), was used in the present study. The ratio of the element concentrations was determined using the ratio of the corresponding areas on the spectrum. The specimen was extruded using a needle from the gasket on the slide plate, broken into fragments, and then deposited on the grid. X-ray diffraction data (XRD) were obtained using an Empyrean PANalytical powder diffractometer (Malvern Panalytical B.V., De Schakel 18, Kamer 50, Eindhoven, 5651 GH, The Netherlands) equipped with a PIXcel3D detector (Bragg-Brentano geometry,  $CuK_{\alpha}$  radiation, step size  $0.0131^{\circ}$ ). For the monochromatization of the primary beam and high intensity of the incident X-ray beam on the sample, we used a Bragg-Brentano HD X-ray optics module (multilayer paraboloid mirror that provided separation of  $K_{\beta}$  radiation and gave the superposition of  $K_{\alpha 1}$  and  $K_{\alpha 2}$ ).

The graphitic-like phase,  $g-C_3N_4$ , was prepared via a solid-state reaction between cyanuric chloride or its fluoro-analog and lithium nitride [19]:



The spherical modification of carbon nitride was obtained when added to a reactor, as a substrate, with nano-size silica spheres, using the procedure described previously [20]. The X-ray diffraction pattern of the starting  $g-C_3N_4$  material is shown in Figure 1. The initial graphite-like  $g-C_3N_4$  is a partially three-dimensional ordered structure, with the following parameters:  $a = 0.2370 \pm 0.0005$  nm and  $c = 0.686 \pm 0.025$  nm, which corresponds to the C-N bond length equal to  $L = 0.137$  nm. This corresponds to the known data described in the literature [4,5,19,21].

According to EELS analysis, the nitrogen concentration in the starting material varied from 23 to 43 at. %. Some lack of nitrogen may be due to the fact that nitrogen deficiency is common in carbon nitrides because of the stability of the easily-formed  $N_2$  molecules [21].

The  $g-C_3N_4$  powder was placed in a 60  $\mu$ m hole of a pre-pressed tungsten gasket without any pressure transmitting media. Pressure was measured from the stress-induced shifts of Raman spectra from a diamond anvil tip [22]. Before loading the  $g-C_3N_4$  specimen, it was kept in a vacuum at a temperature of 95  $^{\circ}$ C for two hours. Three experiments

were conducted with different initial pressure loading levels: (a) 20 GPa; (b) 53 GPa; and (c) 70 GPa. On achieving an initial pressure, shear deformation was applied to the sample by means of rotating one of the anvils around the load axis [17]. At each initial pressure, the anvil was rotated by  $20^\circ$  and returned to its initial position. After applying shear deformation, the pressure increased in the sample to 25, 57, and 79 GPa, accordingly. Pressure increase was induced by a jump in the elastic module and volume [17]. After removing the pressure and extracting the gasket from the diamond cell, the obtained material was examined.

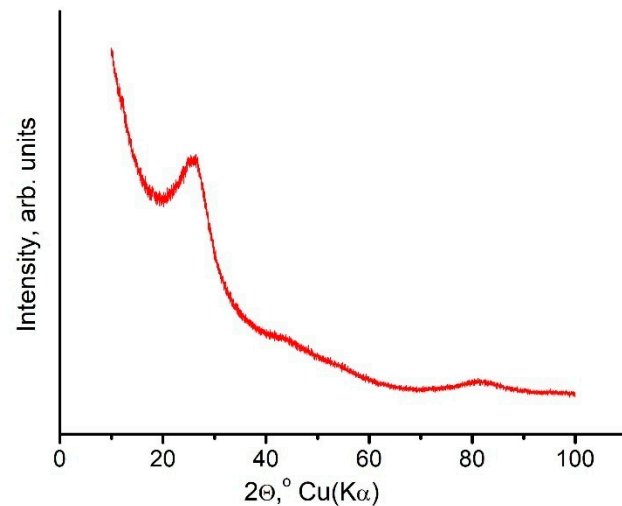
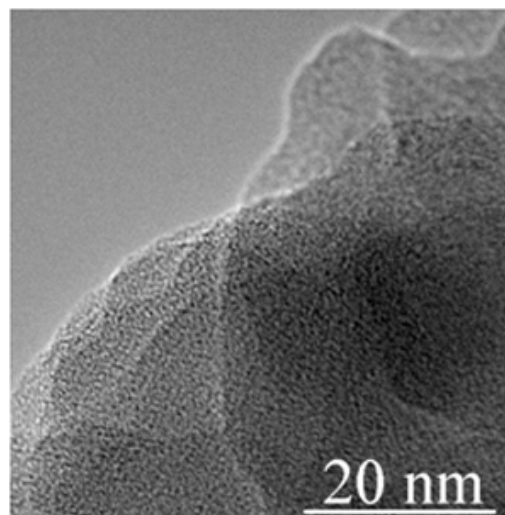


**Figure 1.** The X-ray diffraction pattern of the starting  $g\text{-C}_3\text{N}_4$  material.

### 3. Results

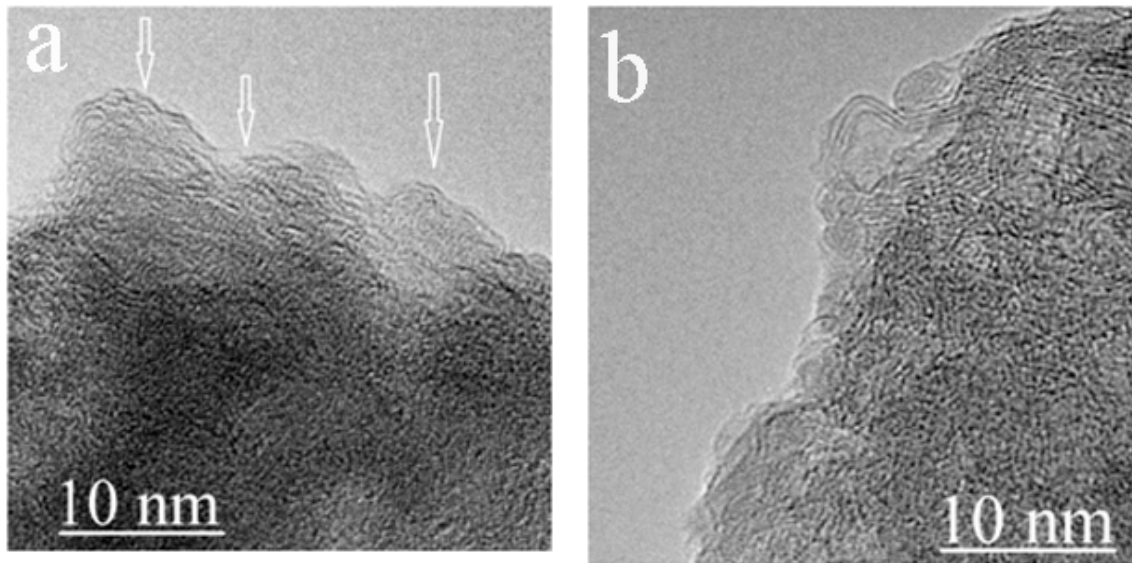
#### 3.1. TEM Study

A TEM image of the starting  $g\text{-C}_3\text{N}_4$  material is shown in Figure 2. The specimen resembles a cluster of amorphous flakes.



**Figure 2.** TEM image of the  $g\text{-C}_3\text{N}_4$  specimen before high-pressure treatment. The specimen resembles a set of amorphous flakes.

After shear deformation at 20–25 GPa, the morphology of the specimen changes. Onion-like structures start to form at the edges of the flakes; their size can be estimated from the TEM image shown in Figure 3 (~5 nm).



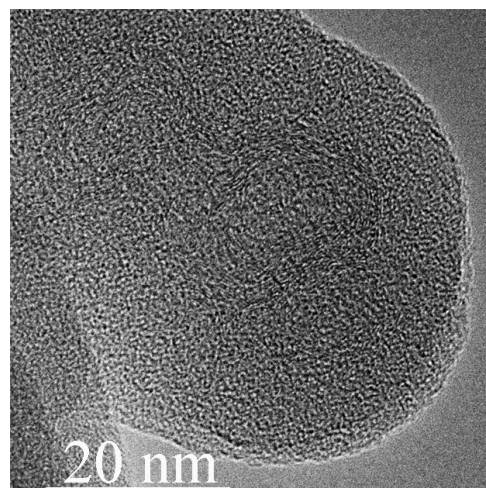
**Figure 3.** TEM images of the  $g\text{-C}_3\text{N}_4$  specimen after shear deformation at 20–25 GPa; (a) an image with graphene-like layers shown by arrows. (b) An image showing an onion-like structure of atypical size.

Table 1 shows the N content after shear deformation is applied at different pressures. We see that after shear deformation, the nitrogen content decreases. Moreover, the higher the pressure before shear deformation, the lower the nitrogen content after deformation. Onion-like structures are also seen in the specimen after being subjected to high shear deformation at 53 GPa.

**Table 1.** Concentrations of carbon and nitrogen in the  $g\text{-C}_3\text{N}_4$  specimen after shear deformation.

Sample	C, at. %	N, at. %
Initial	58	42
20–25 GPa shear	76	24
53–57 GPa shear	93	7
70–79 GPa shear	99	~1

The TEM image of the specimen, after quenching from 57 GPa, is shown in Figure 4. The size of the onion-like fragments increases to 20 nm. Analysis of the EELS spectra demonstrates that the nitrogen content drops to 7% from 42% (Table 1).



**Figure 4.** TEM image of the  $g\text{-C}_3\text{N}_4$  specimen after shear deformation at 53–57 GPa.



Figure 5 shows the TEM images of the specimen quenched from 79 GPa after shear deformation at 70 GPa.

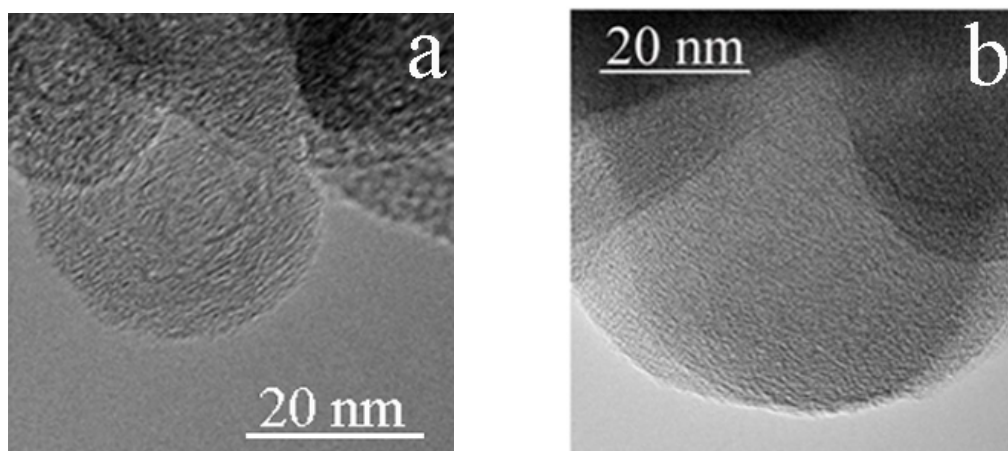


Figure 5. TEM images of different onions (a,b), obtained after shear deformations of the g-C<sub>3</sub>N<sub>4</sub> specimen at 70–79 GPa.

Onion-like structures are seen in the specimen after shear deformation at pressures of 70–79 GPa (Figure 5). The average size of the onion-like structures is still around 20 nm. However, the nitrogen content drops drastically to 1% (Table 1). These data indicate that *sp*<sup>3</sup>-bonded carbon nitride cannot be obtained at 70 GPa under heavy shear deformation.

Three different types of nonoxidized N atoms can be found in C-N materials [23]: (a) “pyridinic”, (b) “pyrrolic”, and (c) “graphitic” nitrogen, with binding energies of ≈399.0, ≈400.3, and ≈401–403 eV, respectively. As follows from the EELS spectra (Figure 6), “graphitic” nitrogen is detected in the C-N phases before and after shear deformation. The presence of strong C-K and N-K  $\pi^*$  peaks indicates that the starting g-C<sub>3</sub>N<sub>4</sub> phase is preferentially *sp*<sup>2</sup> bonded [24,25]. To estimate the concentration of *sp*<sup>2</sup> bonds in the carbon phase, we used the method described in [26]; the results are shown in Table 2. A detailed review of the methods developed for treating the EELS spectra of carbon can be found elsewhere [27].

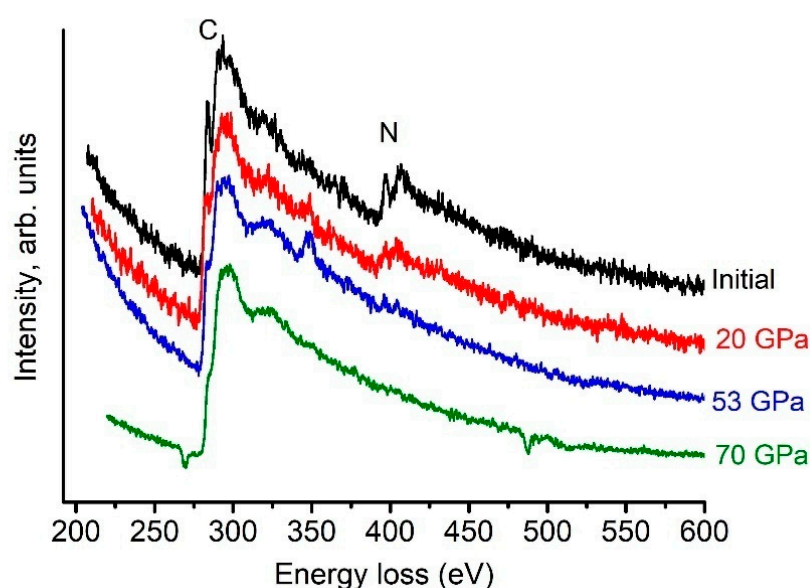


Figure 6. EELS spectra measured on quenched C-N phases. The exposure time when receiving the EELS spectrum is a few seconds. The particle size is several nanometers.

**Table 2.** The  $sp^2$  content using the approach described in Reference [26]. The area under the  $sp^2$  peak (280–285 eV) was divided by the value of the area of the  $sp^3$  peak (286–292 eV). As we can see, the concentration of nitrogen decreases, as well as the concentration of the  $sp^2$  bonds, with increasing pressure in the quenched specimens.

Sample	$sp^2$ Content
Initial	1
20–25 GPa shear	0.92
53–57 GPa shear	0.77
70–79 GPa shear	0.62

### 3.2. Raman Study

Strong fluorescence makes it difficult to measure the Raman spectra of the C-N phases at low pressures [28]. However, a broad band on the Raman spectra can be detected at pressures above 40 GPa. It is centered at  $1730\text{ cm}^{-1}$  at 40 GPa (Figure 7a). We assume that the position of this peak coincides with the  $1620\text{ cm}^{-1}$  peak at an ambient pressure measured in [28] using UV laser. The position of the  $1620\text{ cm}^{-1}$  peak as the function of pressure is shown in Figure 8. The peak positions were found using OriginPro 8 (OriginLab Corporation) tools (OriginLab Corporation, One Roundhouse Plaza, Suite 303, Northampton, MA 01060, United States). The positions are marked in Figure 7. Errors correspond to the symbol size in Figure 8.

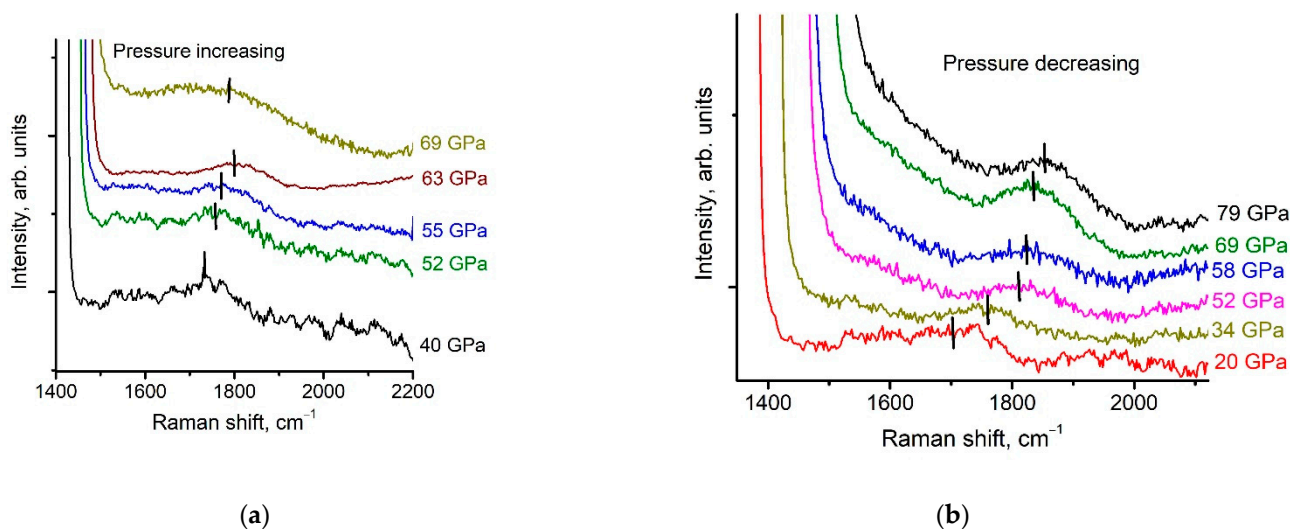


**Figure 7.** The behavior of the Raman spectra of a  $g\text{-C}_3\text{N}_4$  specimen as a function of pressure: (a) increasing pressure, (b) decreasing pressure after shear at 70 GPa.

We denote these curves as  $\nu_g(P)$  curves. Above 40 GPa, the pressure dependence of the  $1620\text{ cm}^{-1}$  peak position can be considered as linear as pressure increases:

$$\nu_g = 1669(13) + 2.432(0.22) \times P \quad (1)$$

It is interesting to compare this behavior with that of graphite above 35 GPa:  $\nu_a = 1669(4) + 0.41(0.06) \times P$  [29]. The difference in slope shape indicates that the graphitic phase is more rigid above 40 GPa. We explain such a difference in rigidity with the fact that graphite transforms into onion-like structures [2,30], whereas the C-N ring keeps its structure in the  $g\text{-C}_3\text{N}_4$  phase. Figure 7b shows that it is possible to trace the  $1620\text{ cm}^{-1}$  peak until 20 GPa, after the application of shear deformation at 70 GPa.

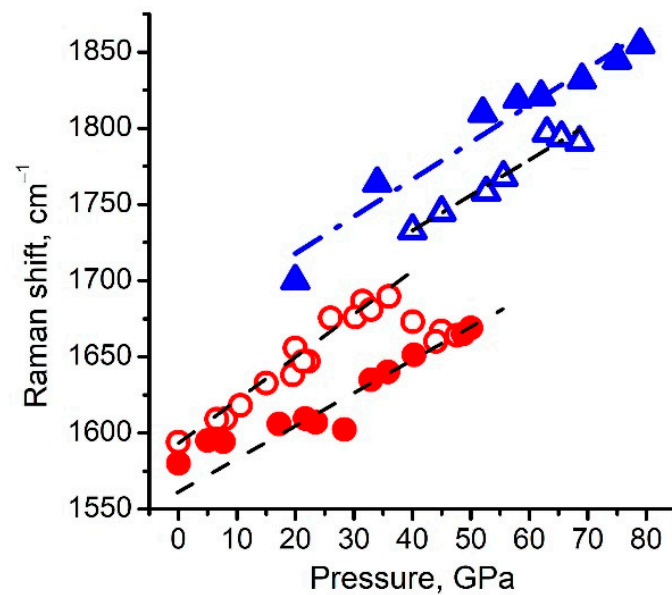


**Figure 8.** Position of the Raman peak of the  $1620\text{ cm}^{-1}$  peak of the  $g\text{-C}_3\text{N}_4$  specimen as a function of pressure: filled triangles for peaks after shear deformation; open triangles for peaks before shear deformation at 70 GPa. Center of the Raman peak of the  $1600\text{ cm}^{-1}$  peak of carbon onions with a diameter of  $\sim 20\text{ nm}$  from Reference [30]; open circles for peaks before deformation; filled circles for peaks after shear deformation.

Below 76 GPa, the pressure dependence of the  $1620\text{ cm}^{-1}$  peak position can be considered as linear, while pressure decreases:

$$\nu_g = 1640(14) + 2.32(0.24) \times P \quad (2)$$

Fluorescence starts growing with decreasing pressure below 20 GPa, and the  $1620\text{ cm}^{-1}$  peak becomes undetectable. As we can see, the slope of the line has not been changed.

Transformation of the  $g\text{-C}_3\text{N}_4$  into 20 nm onion-like structures with low nitrogen contents after shear deformation, at a pressure of 70 GPa, makes it interesting to compare the dependence of the peak at  $\sim 1600\text{ cm}^{-1}$  on pressure for the C-N sample with that of 20 nm pure carbon onions. Carbon onions with a diameter of  $\sim 20\text{ nm}$  were synthesized from natural gas by means of non-catalytic partial oxidation [30].

#### 4. Discussion

One of the main results of this study is that, under shear deformation at high pressures, nitrogen runs away from the carbon structure. Moreover, the higher the pressure, the higher the loss of nitrogen. High-pressure measurements on the graphitic  $\text{C}_3\text{N}_4$  ( $g\text{-C}_3\text{N}_4$ ) phase, using Brillouin light scattering (BLS) up to 41.5 GPa and X-ray Raman scattering (XRS) up to 26 GPa, reveal no structural phase transition and, unlike graphite, no  $sp^2$  to  $sp^3$  rehybridization in this pressure range. It indicates that the loss of nitrogen occurs during shear deformation, which is unexpected as high pressure should make the diffusion of nitrogen atoms difficult. We do not know where the nitrogen atoms go; it is possible that shear deformation leads to the formation of the so-called atomic phase of nitrogen, which is stable under 70 GPa [31] or  $\text{N}_2$  molecules [32]. The severe loss of nitrogen found in this study is not in line with the theoretical predictions [33]. It was predicted that several CN,  $\text{CN}_2$ , and  $\text{C}_3\text{N}_4$  phases would be thermodynamically stable at the pressure range of 14–98 GPa. The behavior of the nitrogen content under high pressure has been studied by several groups. The synthesis of amorphous  $sp^2$ -bonded carbon nitrides at high pressure, from carbon and nitrogen tetracyanoethylene in a DAC at  $2000\text{ }^\circ\text{C}$ , showed that the amount of nitrogen incorporated into the network increases with pressure, ranging from 24% ( $\text{C}_3\text{N}$ ) at 18 GPa

to 38% at 42 GPa ( $C_3N_{1.9}$ ) [24]. Heating turbostratic carbon nitride in the 4.7–17.8 GPa range has revealed the decomposition of t-CN at high temperatures [34]. The onset temperature of t-CN decomposition increases from 990(10) to 1850(50) K. Decomposition results in the formation of disordered graphite at pressures below 8 GPa, and diamond at higher pressures. In our study, we did not observe the formation of the highly incompressible Pnnm CN compound with  $sp^3$ -hybridized carbon, as was synthesized above 55 GPa and 7000 K [10].

Another important result of this study is the first observation of the C-N onion-like structure under pressure. Measurements of the Raman spectrum behavior of the C-N onions under pressure show it to be similar to that of pure carbon onions. To conduct a comparison of the behavior of the carbon onions under pressure with that of the C-N onion-like structure, we loaded the carbon onions into a diamond chamber, following the same procedure as for the C-N sample. Shear deformation was applied at a pressure of 45 GPa (Figure 8). The pressure dependence of the  $1600\text{ cm}^{-1}$  peak position before shear deformation can be considered to be linear as pressure increases:

$$\nu_g = 1605(7) + 1.80(0.26) \times P \quad (3)$$

After shear deformation, the pressure dependence of the  $1600\text{ cm}^{-1}$  peak position can be also considered as linear as pressure decreases:

$$\nu_g = 1576(5) + 1.74(0.17) \times P \quad (4)$$

The abrupt decrease in the frequency of the observed Raman peak from  $1605\text{ cm}^{-1}$  to  $1576\text{ cm}^{-1}$  under pressure in carbon onions, is associated with the formation of an interlayer with  $sp^3$  bonds [30]. We assume that the shift of the  $1600\text{ cm}^{-1}$  peak line in the C-N system is also associated with the formation of the C-N onion-like structure.

Apparently, the partial transformation of  $sp^3$  to  $sp^2$  bonds at  $\sim 15$  GPa during unloading, causes a “jump” in Raman frequency with one linear dependency ( $1560\text{ cm}^{-1}$  at 0 GPa) to another ( $1590\text{ cm}^{-1}$  at 0 GPa) (Figure 7). After the pressure releases, 50% of the  $sp^3$  bonds remain in the samples, according to XPS data [30]. In the Raman spectra, along with the D and G peaks ( $sp^2$  bonds), there is a  $1560\text{ cm}^{-1}$  band ( $sp^3$  bonds). A similar transition of  $sp^2$  to  $sp^3$  hybridization at pressures above 15–20 GPa, and a partial reverse transition when the pressure is released, were also observed in other carbon materials [35–39].

In the case of the C-N sample, the dependence of the Raman band  $\sim 1600\text{ cm}^{-1}$  on pressure was almost the same as for carbon onions. However, up to the maximum pressure in our experiments of 79 GPa, there were no noticeable deviations from linear dependence. At the same time, with increasing pressure, the nitrogen content decreased from 35% to 1% (Table 1). When unloading at a pressure of about 55 GPa, a jump to higher frequencies was observed, as in the case of carbon onions at  $\sim 15$  GPa.

This difference in the behavior of carbon onions and the onion-like structure formed from C-N material at high pressure can be explained using a novel carbon phase diagram [2]. The diagram contains an experimentally revealed zone of diamond instability in the 55–115 GPa pressure range, while at room temperature. Diamond formation stops at these pressures, while the already formed diamonds turn into carbon onions cross-linked by  $sp^3$  bonds. This zone is consistent with the model (based on atomistic modeling) that describes the possible nanostructures as denser than diamond in the 55–100 GPa pressure range [1,2,40]. The results of our study show that the presence of nitrogen in  $sp^3$ -bonded structures, at pressures higher than 55 GPa, reduces the density and, accordingly, carbon structures without nitrogen become thermodynamically favorable. Indeed, the volume of onions cross-linked by  $sp^3$  bonds under a pressure of 70 GPa is  $4.8\text{ \AA}^3/\text{atom}$  [2]. The atomic phase of nitrogen, which is stable under a pressure of 70 GPa [31], has a volume of  $5.8\text{ \AA}^3/\text{atom}$  [41]. A hypothetical compound,  $\beta\text{-C}_3\text{N}_4$  [3,42], has a volume of  $6.2\text{ \AA}^3/\text{atom}$  under ambient conditions. The extrapolation of this value to a pressure of 70 GPa, by analogy with diamond compressibility [42], yields a volume



of  $6.0 \text{ \AA}^3/\text{atom}$ . Consequently, in the case of possible pressure-induced decomposition of  $\beta\text{-C}_3\text{N}_4$  (7 atoms, the volume is  $7\text{atoms} \times 6.0 \text{ \AA}^3/\text{atom} = 42 \text{ \AA}^3$ ), we will observe carbon onions (3 atoms,  $3\text{atoms} \times 4.8 \text{ \AA}^3/\text{atom} = 14.4 \text{ \AA}^3$ ) and the atomic phase of nitrogen (4 atoms,  $4\text{atoms} \times 5.8 \text{ \AA}^3/\text{atom} = 23.7 \text{ \AA}^3$ ). The total volume of the decomposed phases is  $38.1 \text{ \AA}^3$ , which is less than that of  $\beta\text{-C}_3\text{N}_4$  ( $42 \text{ \AA}^3$ ).

## 5. Conclusions

The effect of pressure and shear deformation on amorphous  $\text{C}_3\text{N}_4$  at room temperature leads to the formation of onion-like structures, in which the nitrogen content decreases with increasing pressure (from 42% in the initial sample to 1% in the sample after 80 GPa).

The concentration of  $sp^2$  bonds also decreases from 1 (the initial sample) to 0.62, with increasing pressure to 80 GPa.

The presence of nitrogen in  $sp^3$ -bonded structures at pressures higher than 55 GPa reduces the density and, accordingly, carbon structures without nitrogen become thermodynamically favorable.

**Author Contributions:** V.C., M.P., and P.Z. prepared the samples and performed high-pressure and Raman studies. B.K. and V.B. carried out TEM studies. All the authors have taken part in discussions and the interpretation of the results, and have read and approved the final manuscript. All authors have read and agreed to the published version of the manuscript.

**Funding:** This work in the part of phase transitions study was supported by the Russian Foundation for Basic Research (project 18-29-19019); the part of experiments related to the onion-based material was supported by a grant of the Russian Science Foundation (project #20-12-00097); the work was done using the Shared Research Facilities “Research of Nanostructured, Carbon and Superhard Materials” FSBI TISNCM; M.P. acknowledges the support of the Ministry of Science and Higher Education of the Russian Federation in the framework of the State Task (project code 0718-2020-0037) for Raman study, interpretation, and discussion of obtained results.

**Institutional Review Board Statement:** Not applicable.

**Informed Consent Statement:** Not applicable.

**Data Availability Statement:** The data presented in this study are available on request from the corresponding author.

**Acknowledgments:** The authors thank S.I. Zholudev for X-ray diffraction data and V.N. Khabashesku for graphitic-like material  $g\text{-C}_3\text{N}_4$ .

**Conflicts of Interest:** The authors declare no conflict of interest.

## References

1. Popov, M.Y.; Churkin, V.D.; Kulnitskiy, B.A.; Kirichenko, A.N.; Bulatov, K.M.; Bykov, A.A.; Zinin, P.V.; Blank, V. Transformation of diamond to fullerene-type onions at pressure 70 GPa and temperature 2400 K. *Nanotechnology* **2020**, *31*, 315602. [[CrossRef](#)]
2. Blank, V.D.; Churkin, V.D.; Kulnitskiy, B.A.; Perezhogin, I.A.; Kirichenko, A.N.; Denisov, V.N.; Erohin, S.V.; Sorokin, P.B.; Popov, M.Y. Phase diagram of carbon and the factors limiting the quantity and size of natural diamonds. *Nanotechnology* **2018**, *29*, 115603. [[CrossRef](#)] [[PubMed](#)]
3. Liu, A.Y.; Cohen, M.L. Prediction of new low compressibility solids. *Science* **1989**, *245*, 841–842. [[CrossRef](#)] [[PubMed](#)]
4. Goglio, G.; Foy, D.; Demazeau, G. State of Art and recent trends in bulk carbon nitrides synthesis. *Mater. Sci. Eng. R-Rep.* **2008**, *58*, 195–227. [[CrossRef](#)]
5. Zhao, Z.S.; Xu, B.; Tian, Y.J. Recent Advances in Superhard Materials. In *Annual Review of Materials Research*; Clarke, D.R., Ed.; Annual Reviews: Palo Alto, CA, USA, 2016; Volume 46, pp. 383–406.
6. Horvath-Bordon, E.; Riedel, R.; McMillan, P.F.; Kroll, P.; Miehe, G.; van Aken, P.A.; Zerr, A.; Hoppe, P.; Shebanova, O.; McLaren, I.; et al. High-pressure synthesis of crystalline carbon nitride imide,  $\text{C}_2\text{N}_2(\text{NH})$ . *Angew. Chem.-Int. Ed.* **2007**, *46*, 1476–1480. [[CrossRef](#)] [[PubMed](#)]
7. Fang, L.; Ohfujii, H.; Shinmei, T.; Irifune, T. Experimental study on the stability of graphitic  $\text{C}_3\text{N}_4$  under high pressure and high temperature. *Diam. Relat. Mater.* **2011**, *20*, 819–825. [[CrossRef](#)]
8. Kojima, Y.; Ohfujii, H. Structure and stability of carbon nitride under high pressure and high temperature up to 125 GPa and 3000 K. *Diam. Relat. Mater.* **2013**, *39*, 1–7. [[CrossRef](#)]

9. Sougawa, M.; Takarabe, K.; Mori, Y.; Okada, T.; Yagi, T.; Kariyazaki, H.; Sueoka, K. Bulk modulus and structural changes of carbon nitride C<sub>2</sub>N<sub>2</sub>(CH<sub>2</sub>) under pressure: The strength of C-N single bond. *J. Appl. Phys.* **2013**, *113*. [[CrossRef](#)]
10. Stavrou, E.; Lobanov, S.; Dong, H.F.; Oganov, A.R.; Prakapenka, V.B.; Konopkova, Z.; Goncharov, A.F. Synthesis of Ultra-incompressible spa-Hybridized Carbon Nitride with 1:1 Stoichiometry. *Chem. Mater.* **2016**, *28*, 6925–6933. [[CrossRef](#)]
11. Gao, X.; Yin, H.; Chen, P.W.; Liu, J.J. Shock-induced phase transition of g-C<sub>3</sub>N<sub>4</sub> to a new C<sub>3</sub>N<sub>4</sub> phase. *J. Appl. Phys.* **2019**, *126*, 8. [[CrossRef](#)]
12. Salamat, A.; Woodhead, K.; McMillan, P.F.; Cabrera, R.Q.; Rahman, A.; Adriaens, D.; Cora, F.; Perrillat, J.P. Tetrahedrally bonded dense C<sub>2</sub>N<sub>3</sub>H with a defective wurtzite structure: X-ray diffraction and Raman scattering results at high pressure and ambient conditions. *Phys. Rev. B* **2009**, *80*, 104106. [[CrossRef](#)]
13. Ming, L.C.; Zinin, P.; Meng, Y.; Liu, X.R.; Hong, S.M.; Xie, Y. A cubic phase of C<sub>3</sub>N<sub>4</sub> synthesized in the diamond-anvil cell. *J. Appl. Phys.* **2006**, *99*, 033520. [[CrossRef](#)]
14. Goncharov, A.F. Graphite at high pressures: Amorphization at 44 GPa. *High Press. Res.* **1992**, *8*, 607–616. [[CrossRef](#)]
15. Aksenenkov, V.V.; Blank, V.D.; Borovikov, N.F.; Danilov, V.G.; Kozorezov, K.I. Production of diamond single crystals in graphite under plastic deformation. *Physics-Doklady* **1994**, *39*, 700–703.
16. Bridgman, P.W. Effects of High Shearing Stress Combined with High Hydrostatic Pressure. *Phys. Rev.* **1935**, *48*, 825–847. [[CrossRef](#)]
17. Blank, V.D.; Popov, M.Y.; Kulnitskiy, B.A. The Effect of Severe Plastic Deformations on Phase Transitions and Structure of Solids. *Mater. Trans.* **2019**, *60*, 1500–1505. [[CrossRef](#)]
18. Popov, M.; Koga, Y.; Fujiwara, S.; Mavrin, B.N.; Blank, V.D. Carbon nanocluster-based superhard materials. *New Diam. Front. Carbon Technol.* **2002**, *12*, 229–260.
19. Khabashesku, V.N.; Zimmerman, J.L.; Margrave, J.L. Powder synthesis and characterization of amorphous carbon nitride. *Chem. Mater.* **2000**, *12*, 3264–3270. [[CrossRef](#)]
20. Zimmerman, J.L.; Williams, R.; Khabashesku, V.N.; Margrave, J.L. Synthesis of spherical carbon nitride nanostructures. *Nano Lett.* **2001**, *1*, 731–734. [[CrossRef](#)]
21. Foy, D.; Demazeau, G.; Florian, P.; Massiot, D.; Labrugère, C.; Goglio, G. Modulation of the crystallinity of hydrogenated nitrogen-rich graphitic carbon nitrides. *J. Solid State Chem.* **2009**, *182*, 165–171. [[CrossRef](#)]
22. Popov, M. Pressure measurements from Raman spectra of stressed diamond anvils. *J. Appl. Phys.* **2004**, *95*, 5509–5514. [[CrossRef](#)]
23. Casanovas, J.; Ricart, J.M.; Rubio, J.; Illas, F.; Jiménez-Mateos, J.M. Origin of the Large N 1s Binding Energy in X-ray Photoelectron Spectra of Calcined Carbonaceous Materials. *J. Am. Chem. Soc.* **1996**, *118*, 8071–8076. [[CrossRef](#)]
24. Nesting, D.C.; Badding, J.V. High-pressure synthesis of sp(2)-bonded carbon nitrides. *Chem. Mater.* **1996**, *8*, 1535–1539. [[CrossRef](#)]
25. Rodil, S.E.; Muhl, S. Bonding in amorphous carbon nitride. *Diam. Relat. Mater.* **2004**, *13*, 1521–1531. [[CrossRef](#)]
26. Jimenez, I.; Gago, R.; Albella, J.M.; Caceres, D.; Vergara, I. Spectroscopy of pi bonding in hard graphitic carbon nitride films: Superstructure of basal planes and hardening mechanisms. *Phys. Rev. B* **2000**, *62*, 4261–4264. [[CrossRef](#)]
27. Lajaunie, L.; Pardanaud, C.; Martin, C.; Puech, P.; Hu, C.; Biggs, M.J.; Arenal, R. Advanced spectroscopic analyses on a:C-H materials: Revisiting the EELS characterization and its coupling with multi-wavelength Raman spectroscopy. *Carbon* **2017**, *112*, 149–161. [[CrossRef](#)]
28. Zinin, P.V.; Ming, L.C.; Sharma, S.K.; Khabashesku, V.N.; Liu, X.R.; Hong, S.M.; Endo, S.; Acosta, T. Ultraviolet and near-infrared Raman spectroscopy of graphitic C<sub>3</sub>N<sub>4</sub> phase. *Chem. Phys. Lett.* **2009**, *472*, 69–73. [[CrossRef](#)]
29. Otake, S.; Zinin, P.V.; Hellebrand, E.; Prakapenka, V.; Liu, Y.S.; Hong, S.M.; Burgess, K.; Ming, L.C. Formation of the high pressure graphite and BC8 phases in a cold compression experiment by Raman scattering. *J. Raman Spectrosc.* **2013**, *44*, 1596–1602. [[CrossRef](#)]
30. Lugvishchuk, D.S.; Mitberg, E.B.; Kulnitskiy, B.A.; Skryleva, E.A.; Parkhomenko, Y.N.; Popov, M.Y.; Churkin, V.D.; Mordkovich, V.Z. Irreversible high pressure phase transformation of onion-like carbon due to shell confinement. *Diam. Relat. Mater.* **2020**, *107*, 7. [[CrossRef](#)]
31. Popov, M. Raman and infrared study of high-pressure atomic phase of nitrogen. *Phys. Lett. A* **2005**, *334*, 317–325. [[CrossRef](#)]
32. Houska, J. Maximum N content in a-CN<sub>x</sub> by ab-initio simulations. *Acta Mater.* **2019**, *174*, 189–194. [[CrossRef](#)]
33. Dong, H.F.; Oganov, A.R.; Zhu, Q.; Qian, G.R. The phase diagram and hardness of carbon nitrides. *Sci. Rep.* **2015**, *5*, 5. [[CrossRef](#)] [[PubMed](#)]
34. Solozhenko, V.; Solozhenko, E.; Zinin, P.; Ming, L.; Chen, J.; Parise, J. Equation of State and Phase Stability of Turbostratic Carbon Nitride. *J. Phys. Chem. Solids* **2003**, *64*, 1265–1270. [[CrossRef](#)]
35. Pashkin, E.Y.; Pankov, A.M.; Kulnitskiy, B.A.; Perezhogin, I.A.; Karaeva, A.R.; Mordkovich, V.Z.; Popov, M.Y.; Sorokin, P.B.; Blank, V.D. The unexpected stability of multiwall nanotubes under high pressure and shear deformation. *Appl. Phys. Lett.* **2016**, *109*, 081904. [[CrossRef](#)]
36. Yao, M.; Fan, X.; Zhang, W.; Bao, Y.; Liu, R.; Sundqvist, B.; Liu, B. Uniaxial-stress-driven transformation in cold compressed glassy carbon. *Appl. Phys. Lett.* **2017**, *111*, 101901. [[CrossRef](#)]
37. Yang, X.; Yao, M.; Wu, X.; Liu, S.; Chen, S.; Yang, K.; Liu, R.; Cui, T.; Sundqvist, B.; Liu, B. Novel Superhard sp<sup>3</sup> Carbon Allotrope from Cold-Compressed C<sub>70</sub> Peapods. *Phys. Rev. Lett.* **2017**, *118*, 245701. [[CrossRef](#)] [[PubMed](#)]

38. Shiell, T.B.; de Tomas, C.; McCulloch, D.G.; McKenzie, D.R.; Basu, A.; Suarez-Martinez, I.; Marks, N.A.; Boehler, R.; Haberl, B.; Bradby, J.E. In situ analysis of the structural transformation of glassy carbon under compression at room temperature. *Phys. Rev. B* **2019**, *99*, 024114. [[CrossRef](#)]
39. Pankov, A.M.; Bredikhina, A.S.; Kulnitskiy, B.A.; Perezhogin, I.A.; Skryleva, E.A.; Parkhomenko, Y.N.; Popov, M.Y.; Blank, V.D. Transformation of multiwall carbon nanotubes to onions with layers cross-linked by sp<sup>3</sup> bonds under high pressure and shear deformation. *AIP Adv.* **2017**, *7*, 085218. [[CrossRef](#)]
40. Blank, V.D.; Churkin, V.D.; Kulnitskiy, B.A.; Perezhogin, I.A.; Kirichenko, A.N.; Erohin, S.V.; Sorokin, P.B.; Popov, M.Y. Pressure-Induced Transformation of Graphite and Diamond to Onions. *Crystals* **2018**, *8*, 68. [[CrossRef](#)]
41. Barbee, T.W. Metastability of atomic phases of nitrogen. *Phys. Rev. B* **1993**, *48*, 9327–9330. [[CrossRef](#)] [[PubMed](#)]
42. Teter, D.M.; Hemley, R.J. Low-Compressibility Carbon Nitrides. *Science* **1996**, *271*, 53. [[CrossRef](#)]